Effects of lubricant oil on particulate emissions from port-fuel and direct-injection spark-ignition engines

Effects of Lubricant Oil on Particulate Emissions from Port Fuel and Direct Injection Spark-Ignition Engines

Amirante, Riccardo; Politecnico di Bari, Department of Mechanics, Mathematics and Management

Distaso, Elia; Politecnico di Bari, Department of Mechanics, Mathematics and Management

DI IORIO, SILVANA; ISTITUTO MOTORI-CNR,

Napolitano, Michele; Politecnico di Bari, Department of Mechanics, Mathematics and Management

SEMENTA, PAOLO; Istituto Motori CNR,

Tamburrano, Paolo; Politecnico di Bari, Department of Mechanics, Mathematics and Management

Vaglieco, Bianca Maria; Istituto Motori, Reitz, Rolf; University of Wisconsin-Madison, Mechanical Engineering

ABSTRACT

This work presents experimental tests where lubricant oil was added to the engine in order to highlight its contribution to particle emissions from both gasoline and Compressed Natural Gas (CNG) Spark-Ignition (SI) engines. Three different ways of feeding the extra lubricant oil and two fuel injection modes – Port Fuel Injection (PFI) and Direct Injection (DI) – were investigated to mimic the different ways by which lubricant may reach the combustion chamber. In particular, in the tests using CNG, the oil was injected either into the intake manifold or directly into the combustion chamber, whereas in both the PFI and DI tests using gasoline, the oil was premixed with the fuel. The experiments were performed on a single-cylinder, optically accessible SI engine, running at 2000 rpm under stoichiometric and full load conditions, and requiring no lubrication. Particle Size Distribution (PSD) functions were measured in the range from 5.6 to 560 nm by means of an Engine Exhaust Particle Sizer. Particle samples were taken directly from the exhaust flow, just downstream of the valves. Opacity was measured by an AVL 439 Opacimeter and gaseous emissions were measured by means of an exhaust gas analyzer in order to globally monitor the combustion process. Detailed analysis of the recorded total Particulate Number and PSDs allowed to determine the size ranges and relative amounts associated with the lubricant-oil-derived particles. Oil addition produced a significant increase of the particles emitted in the lowest range-size, independently of the way lubricant was added. Only when lubricant was injected directly into the combustion chamber (either blended with the fuel, or by itself), an increase in the number of particles with sizes larger than 50 nm was recorded.

1. INTRODUCTION

Modern engine technologies are subject to increasingly tighter emission standards and must achieve consistently lower particulate emission levels. Therefore, an increasing attention has been focused on developing new reduction strategies, such as implementing innovative combustion-control techniques [1][2], coupled with various after-treatment devices [3]. A few years ago, only the Particulate Matter (mass) (PM) was measured, which parameter in no longer adequate for today's low emission levels [4], insofar as the fine particles account very little for particle mass, but can contribute significantly to the Particulate Number (PN). And in fact stringent limits for PN-concentration have been introduced in order to reduce the unhealthy effects resulting from inhalation of very fine particles, believed to cause more damage than larger ones [5][6][7][8][9]. For the reasons above, a great research effort is being made worldwide to better understand the production mechanisms of such emissions so as to meet PN-based regulations. In particular, the influence of engine lubricant on particulate emission is still unclear, so that elucidating the mechanisms of oil-derived soot formation can play an important role towards reducing fuel-derived particulate emissions as well as developing new lubricant oil formulations, until cleaner emerging technologies will be ready for the transportation marketplace [10][11][12][13].

Engine lubricant oil is composed of a base oil and an additive package. In general, the base oil is composed of petroleum-derived mineral oils, whereas the additive package is composed of various chemicals, including metal compounds (such as Ca, Ba, Mg, Fe, Ni, Mn, Cu and Zn) [14][15]. Metals traces derived from the lubricant oil can thus be found in the exhausts of both SI and Diesel engines [16] [17][18][19]. More insight into lubricant oil contribution to particle emissions is thus needed since health hazard produced by exposure to nanoparticles increases with their metal content [20][21][22]. Moreover, the toxic activity of exhausts is strongly associated with traces of lubricant oil emissions, such as Zn, P, Ca, suggesting that the incomplete combustion of lubricant oil leads to increased health risks [18].

Early studies about the oil contribution to the particle emission were focused on modern Diesel engines, in which the oxidation catalyst and the Diesel Particulate Filter (DPF) reduce the organic and inorganic (soot and metals) fractions of the lubricant-oil PM [16], respectively. A study by McGeehan et al. [17] has shown that the ashes deposited in the DPF of a Diesel engine are predominantly inorganic and dominated by lubricant oil additives. In SI engines, the contribution of lubricant oil to tailpipe PM can be significant, because the Three-Way Catalyst (TWC) oxidizes the organic fraction of the PM, but there is no DPF to remove the inorganic soot and metal traces [16].

In addition, several studies [23][24][25] have shown that, in Diesel engines, metal additives may reduce the accumulation mode while increasing the nucleation one. Jung et al. [26] showed that metals in lubricant-oil blended with fuel might play a similar role, by investigating the influence of metals on soot oxidation and particle emissions using lubricant oil-dosed fuel (2% by volume). Their PSD measurements showed that particle volume emissions, which are roughly proportional to particle mass, decreased by about a factor of two with dosed fuel, whilst PN emissions—mostly solid nuclei-mode particles below 30 nm—increased by an order of magnitude.

Miller et al. [27] demonstrated that the metal traces emitted by SI engines are derived mainly from the combustion of lubricant oil, by using a modified CAT 3304 Diesel engine fueled with hydrogen. The compression ratio of the engine was reduced from 15 to 12 and an SI system and a turbocharger with aftercooler were added to it. The engine produced exhaust aerosol with log normal-size distributions with (geometric) mean diameters ranging from 18 to 31 nm. The particles contained some organic compounds, little or no elemental carbon, and a much larger percentage of metals than particles from the original engine. These results indicate that the results obtained on Diesel engines [23][25][24] can be extended to SI engines and are in agreement with those of Thiruvengadam et al. [16].

More recently, Sonntag et al. [28] estimated that the contribution of lubricant oil to the PM emissions can be around 25% in gasoline engines. Pirjola et al. [29] studied particle emissions from a modern turbocharged gasoline DI passenger car engine while the vehicle was running with five different lubricant oils. Their results highlighted that particle emissions during transient operation strongly depend on the lubricant oil and a 78% reduction in PN emissions was observed solely by changing its properties.

Therefore, investigating the ways by which lubricant oil can reach the exhausts is crucial to understand how lubricant oil can influence particle formation. Indeed, it is well known that lubricant oil is continuously consumed in the combustion chamber and, in some cases, it can provide the greatest contribution to the exhaust PM, even though it amounts to only about 0.2% of the fuel consumption [26], or even 0.1% for today's engines [30]. For instance, metals that form solid particles can come from lubricant oil that is spread onto the cylinder walls by the piston rings or that flows into the combustion chamber from the top-ring groove [31]. In addition, the design of the cylinder head-liner block structure allowing locally differing deformations of the liner under pressure plays a primary role in determining one of the most important escape routes. Other main routes are represented by the turbocharger seals, the valve stem seals, and the positive crankcase ventilation system [30]. However, due to the complexity of the phenomenon, it is still not entirely clear which mechanism contributes most to oil consumption.

Moreover, it has to be considered that lubricant oil may leave the cylinder walls by either vaporization or atomization. De Petris et al. [31] showed that oil mist (or oil atomized by a reverse blow-by) was a main contributor to oil consumption under their test conditions. The escape route is equally critical in determining the extent of oxidation: for example, a small leak through the exhaust valve generates more particulate than a much larger one through the inlet valve, simply because the oil is oxidized less effectively [30].

Finally, engine operation largely affects oil consumption, in particular during accelerations [16][32]. Yilmaz et al. [32] measured a sudden increase of oil consumption during transients from low to high load-conditions: oil consumption reached a peak and then gradually decreased to the much lower steady state level of the final operating condition. The increase in oil consumption seen during accelerations is reasonably associated with—and somewhat explains—the large number of nucleation-mode particles released from CNG SI engines during accelerations [33][34][35], in particular after long idling periods [36].

The aim of the present study is to provide more insight into the effects of lubricant oil on particle emissions from both gasoline and CNG SI engines, by means of an experimental campaign designed for this very purpose. Both direct- and port-injection modes were investigated. The results demonstrate the formation of particles produced solely from lubricant oil, and help ascertain the concentration number and size distribution of lubricant-oil-derived particles. The strategy adopted in emulating the possible ways by which lubricant oil can reach the combustion chamber was inspired by the technique used in a well-known work by Stanglmaier et al. [37]: a controlled amount of liquid fuel was deposited on a given location within the combustion chamber at a desired crank angle by means of a spark-plug-mounted directional-injection-probe so that the HC emissions due to in-cylinder wall wetting could be studied independently of all other HC sources. Since in a comparable context it was recognized to be a valid method, a similar approach was adopted in the present study. Thus, for the first time, lubricant oil contribution to the particle emission was investigated by means of external oil injection within an engine running without any lubrication. The effects on particle emissions when lubricant oil was blended into the fuel were studied too. Both direct and indirect lubricant oil injections were performed.

2. EXPERIMENTAL METHOD

2.1. Apparatus

The experimental apparatus included the SI engine later described in detail, an electrical dynamometer, a CNG injection line, a gasoline injection line, a dedicated oil injection line, a three-hole commercial low pressure gasoline injector, a single-hole Natural Gas Injector (NGI), a seven-hole commercial high-pressure gasoline injector, the data acquisition and control units and four emission measurement systems. The engine was fueled with commercial European gasoline and with CNG. The gasoline chemical and physical properties are listed in Table 1, while the composition of the natural gas is reported in Table 2; the properties of the two fuels were provided by the suppliers.

Table 1 Chemical and physical properties of gasoline.

Name	Units	Value
Carbon	mass%	86.12
Hydrogen	mass%	13.25
Oxygen	mass%	0.63
Aromatic content	%v/v	35.00
Density - at 15 °C -	kg/l	0.75
Viscosity - at 20 °C -	mPa*s	0.39
LHV	MJ/l	32.00
Stoichiometric air/fuel	None	14.70
Motor Octane number	Rating	84.20
Research Octane number	Rating	94.50

Table 2 Natural gas chemical composition.

Name	Fraction
Carbon dioxide (CO_2)	1 %
Nitrogen (N_2)	2 %
Methane (CH_4)	88 %
Ethane (C_2H_6)	2 %
Propane (C_3H_8)	7 %

Table 3 Engine specifications.

Name	Units	Value
Cylinder volume	cm^3	250
Bore	mm	72
Stroke	mm	60

Compression ratio	None	10.5
Max power	kW	16 at 8000 rpm
Max torque	Nm	20 at 5500 rpm

The injection and ignition parameters, were set by means of a programmable electronic unit. A linear lambda sensor Bosch LSU 4.9 installed at the exhaust was used to measure the air-fuel ratio. The fuel Duration Of Injection (DOI) was properly adjusted by a closed-loop control on the lambda value to obtain a stoichiometric equivalence ratio. The in-cylinder pressure was measured by means of a quartz pressure transducer flush-mounted in the region between the intake and exhaust valves and having a sensitivity of 19 pC/bar and a natural frequency of 130 kHz. The electrical dynamometer allowed the operation under both motoring and firing conditions.

2.1.1. Engine

A 4-stroke, single cylinder, SI, optically accessible engine, with specifications shown in

Table 3 and not equipped with any after-treatment device was used in all tests at 2000 rpm and full load. The spark plug was centrally located in the engine head. The engine could run in both Direct Injection (DI) and Port Fuel Injection (PFI) modes, and also without lubrication [38]. A six-hole high pressure direct injector was located between the intake valves. The intake duct was equipped with both a three-hole commercial low-pressure injector and a natural gas single-hole injector.

2.1.2. Emission measurement systems

PN concentrations and sizes were measured in the range from 5 to 560 nm by means of a TSI Engine Exhaust Particle Sizer. The exhausts were sampled and diluted by means of the Dekati Engine Exhaust Diluter, according to the Particle Measurement Programme (PMP). The dilution ratio was fixed at 1:79. A 1.5 m heated line was used for sampling the engine exhausts in order to avoid condensation of combustion water. The sample is first diluted with air heated above 150 °C. Then, the sample passes through an evaporation chamber at a temperature above 300 °C for removing volatile particles. This system allows to measure the solid particles defined by the PMP as particles that can survive passing through an Evaporation Tube with a wall temperature of 300–400 °C. Samples for the particle characterization were taken directly from the exhausts, shortly after leaving the cylinder.

CO, CO_2 and HC emissions were measured by means of non-dispersive infrared detectors; NO_x were detected by means of electrochemical sensors. Opacity [%] was continuously measured by an AVL 439 Opacimeter. Methane-HC emissions were measured by means of a Flame Ionization Detector.

2.2. Experimental procedure

The present work focused on the formation of soot particles derived solely from lubrication oil and, through the analysis of the number concentration and PSD functions, helped to isolate the size ranges and the amounts of lubricant-oil-derived particles. Therefore, the tests were performed at the "Istituto Motori CNR", Italy, which has adequate facilities.

Eastwood [30] summarized the relevance of engine lubricant for particulate emission as: "*Investigations in which oil consumption is increased deliberately, by artificial means, might be relying on precarious assumptions as to the combustion mode of this oil. These remarks highlight the need to learn much more about the combustion of escaping lubricant."* This statement is related to what Sutton et al. [39] observed when a lubricant-fuel mixture is burned: the resulting ash differs in its morphology from that observed when lubricant is instead entrained into the air intake as a mist.

In light of these considerations, three different ways of providing the excess lubricant oil and two injection modes (PFI and DI) were investigated. When gasoline was used as fuel, a lubricant-fuel mixture was prepared and then injected in either port or direct mode, allowing to study how the injection mode impacts the soot formation dynamics. When the engine was fueled with CNG, always port injected, the oil was either entrained into the intake manifold or directly into the combustion chamber. In the latter case, a relatively large amount of lubricant was released for a very short time (the oil injection, lasting only 30 CADs, lasted less than 12 engine cycles, namely, about 0.7 s). This procedure aimed at emulating the droplet escape from the valve stem seals directly into the combustion chamber.

By these means, it was possible to observe the lubricant contribution to particle emissions with the oil both separately injected into the intake and directly into the combustion chamber, as well as supplied as “additive” to the fuel, when the latter is provided to the engine both within the intake manifold and directly into the combustion chamber.

In the present experiments, with the purpose of clearly isolating the lubricant contributions, we chose to start from a level of the oil-to-fuel mass equal to 1%, representative of transient operating conditions [32], in which the oil contributes most to particle emissions [33][34][35][36]. Then, oil-to-fuel mass fractions equal to 3, 5 and 7% were used to investigate how PN and sizes relate to the amount of oil entering the combustion chamber.

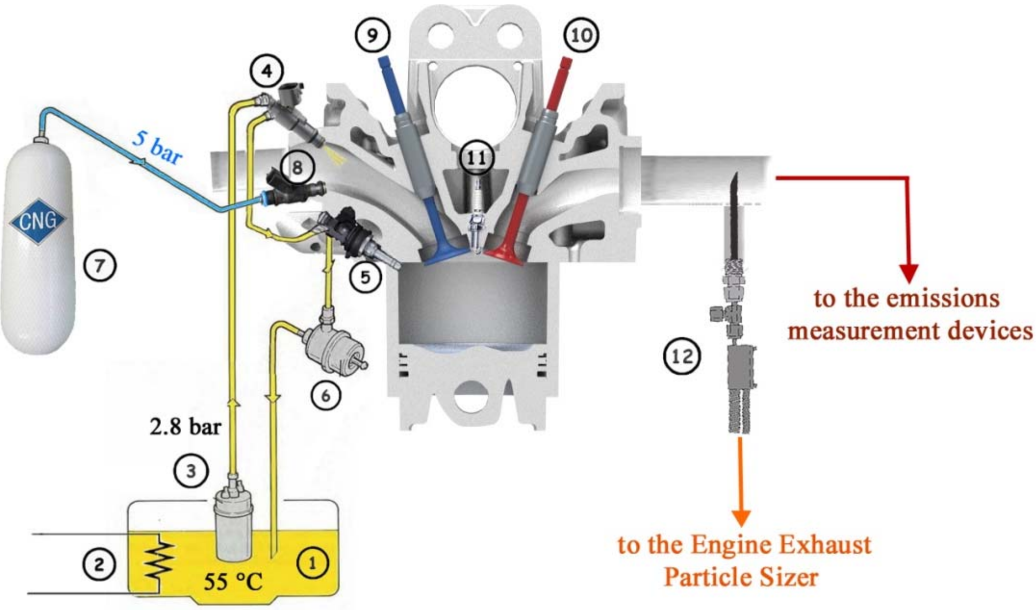

Figure 1. Experimental Set-up for the CNG tests. (1) Oil tank; (2) resistors for heating the oil to 55 °C; (3) oil pump; (4) 3-hole commercial low pressure injector; (5) 6-hole commercial high-pressure injector; (6) oil pressure regulator; (7) CNG bottle; (8) CNG 1-hole injector; (9) intake and (10) exhaust valves; (11) spark-plug; (12) particle sizer probe.

Table 4. Physical and chemical lubricant oil characteristics (Castrol© EDGE 0W-30 technical datasheet).

Name	Method	Units	Value
Density @ 15 °C, Relative	ASTM D4052	g/ml	0.842
Viscosity, Kinematic 100 °C	ASTM D445	mm^2/s	12.3
Viscosity, CCS -35C (0W)	ASTM D5293	mPa.s (cP)	5800
Viscosity, Kinematic 40 °C	ASTM D445	mm^2/s	72
Viscosity Index	ASTM D2270	None	169
Pour Point	ASTM D97	°C	-51
Flash Point, PMCC	ASTM D93	°C	200
Ash, Sulphated	ASTM D874	%wt	0.8
Distillates (petroleum), hydro-treated heavy paraffinic	CAS: 64742-54-7	%	>=75 - <90
Lubricant oils (petroleum), C20-C50, hydro-treated neutral oil-based	CAS: 72623-87-1	%	<10

2.2.1. CNG tests

Figure 1 shows a schematic representation of the experimental set-up for CNG tests. The gaseous fuel was supplied by a pressurized bottle using a pressure regulator typically set to 5 bar. The CNG single-hole injector (number 8 in Figure 1) was used for the natural gas injection. When the oil was injected into intake manifold, a three-hole commercial low-pressure gasoline injector was used (number 4 in Figure 1). In the droplet-emulation tests, in which oil is directly injected into combustion chamber, the six-hole high-pressure commercial injector (number 5 in Figure 1) was employed.

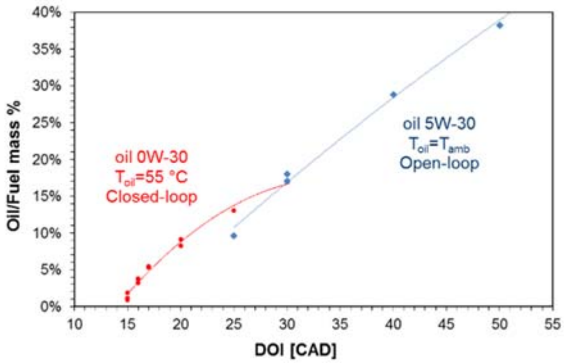

Figure 2. Three-hole oil Injector characterization with two different set-ups. The injected mass flow rate is normalized by the fuel mass flow rate.

The oil injection line is depicted in yellow in Figure 1. This arrangement achieved the greatest precision in matching the lowest values of the injected oil mass. Heating the oil to 55 °C allowed a decrease in viscosity (and density), which strongly depends on the temperature (especially below the usual temperature working conditions). It is known that the viscosity of a fluid lubricant affects friction. The addition of a return circuit ensured continuous oil motion into the pipes (especially near the injector nozzle) and avoided oil cooling which might lock the injection at the lowest DOI. A pressure regulator (number 6 in Figure 1) was used to set and monitor the oil injection pressure at 2.8 bar, which is a reasonable compromise between the small flow rate required and the proper injector operation.

The oil used in the experiments was a commercial, multi-grade, low viscosity, full-synthetic lubricant 0W-30. Its main physical and chemical characteristics, as provided by the supplier, are listed in Table 4.

It was essential to characterize the injector behavior at the lowest injected flows, since a small amount of injected oil was the desired target. Figure 2 reports the results obtained using two different configurations. The red line refers to the earlier described arrangement, while the blue line was obtained without the oil return circuit and by injecting a slightly different oil (a 5W-30 of a different supplier) at room temperature. In this case, it was not possible to inject less than 10% of the fuel mass flow rate, which is disproportionately larger than the selected minimum value of 1%. This highlighted how difficult can be injecting such small oil amounts whit the required precision. Therefore, the experimental set-up of Figure 1 was used during the whole experimental campaign.

Since the optical engine can run without requiring any lubrication, it was possible to obtain zero-oil baseline measurements. However, the length of each test had to be short to avoid damage to the self-lubricating teflon-bronze composite piston rings. The extra-oil injected fouls the optical access, without increasing the lubrication effect. Short combustion durations can be a problem in reaching stable measurements. In Figure 3 (a) a typical observed total number concentration behavior of the emitted particles during a test with natural gas and 1% of oil continuously injected into intake manifold is reported. The number of the detected particles increased as soon as combustion started and kept increasing until it ended, and the size distribution also kept changing. Thus, it was not possible to reach a steady state condition before the end of combustion by using a standard oil injection strategy. It was supposed that, the oil impacted the intake manifold walls and a film formed, so that the oil amount carried by the intake air flow increased constantly together with the number of particles detected at the exhausts. In order to avoid this drawback and reach steady conditions just as the combustion started, lubricant oil injection was started about one and half minutes before the combustion, while the engine was motored. This allowed the film thickness to stabilize before the start of the test, as shown in Figure 3 (b). No appreciable fluctuation was visible in this case during the combustion period. This approach was used in all CNG tests with oil entrained into the intake manifold.

In all tests, the CNG at stoichiometric conditions was injected for 115 CADs, ending at TDC, and ignition was triggered at 24 CADs.

2.2.2. Gasoline tests

In gasoline tests the oil was always mixed with the fuel; four different oil-gasoline mixtures were used and both the PFI and DI strategies were adopted. In the PFI case, the three-hole commercial low-pressure injector (placed in position 4 in Figure 1) was used. In the DI case, the six-hole high-pressure commercial injector (located in position 5 in Figure 1) was used to inject either the gasoline or the mixture of oil-gasoline directly into the combustion chamber. In the latter case, the gasoline was injected at a pressure of 100 bar using an additional high-pressure pump. When the PFI mode was employed, steady conditions were not reached just as in the case of CNG tests and the same motoring strategy was again used with success.

For a better comparison with CNG tests, stoichiometric conditions were always enforced and ignition was again triggered at 24 CADs before TDC, which allowed a stable and efficient combustion in all tests.

During the PFI mode, gasoline was injected for 120 CADs and the injection ended 230 CADs before TDC. During the DI mode, an early Injection was adopted, starting 285 CADs before TDC and lasting about 35 CADs.

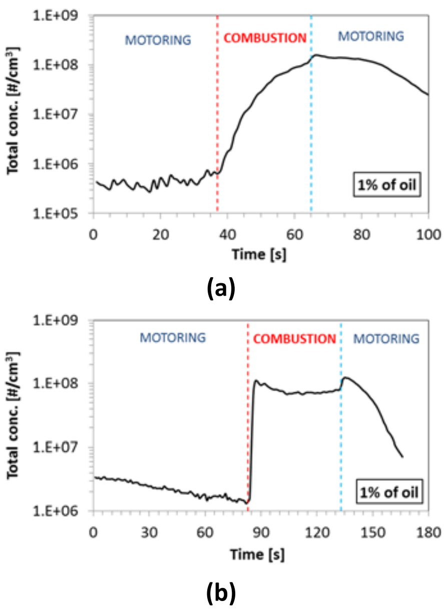

Figure 3 Total PN concentration measurements for CNG test with 1% of oil without (a) and with (b) "film-strategy". Red dashed line: start of combustion; light blue dashed line: end of combustion.

3. RESULTS AND DISCUSSION

The results obtained in the PFI mode for both the CNG and gasoline tests are described first. Then, we examine those obtained when the oil-gasoline mixture as well as the lubricant oil alone were injected directly into the combustion chamber.

3.1. PFI mode

In order to achieve a reasonable statistical validity, several repetitions of each test were carried out, and the derived mean values for each test were used for the comparisons. In each graph of Figure 4 all available repetitions of each single test are shown for both CNG and gasoline. This comparison, besides providing statistical validation of the results, highlights the fact that no appreciable differences were seen between the two different ways in providing the excess lubricant from the PN point of view.

Figure 5 shows the total concentration number evolution with time for representative tests for each oil percentage considered. In Figure 6 the corresponding granulometric distributions are depicted. By looking at Figure 5 it is possible to appreciate that all the combustion measurements were stable, and had very low variability. This is also appreciable from the 95% confidence interval reported for each distribution (red lines) in Figure 6. It is also interesting to notice that as soon as the amount of the injected lubricant oil starts to be very large (Figure 5 (d) and (e) for CNG and (δ) and (ε) for gasoline), the PN started to increase during motoring conditions that preceded the combustion period. Thus, it might be reasonable to suppose that the film formation process on the intake manifold walls could be effectively taking place. This aspect appears distinguishable since the oil is 3% of the CNG injected mass (Figure 5 (c)) and even when oil is at 1% for the gasoline tests (Figure 5 (β)).

A direct comparison between the mean values reported in Figure 4 summarizes these observations. Figure 7 uses two different scales to provide a global and detailed view at the same time. If a linear scale is chosen (see Figure 7 (a) and (α)), it is not possible to see the baseline zero-oil curve because it is roughly two-orders of magnitude below the value range of the data. Conversely, if the data are plotted along a logarithmic scale, details about the peaks are lost. The level of PN measurable when burning natural gas is so low as to be very close to the level recorded during motoring conditions, as seen from Figure 6 (a). The values recorded with gasoline are low too (Figure 6 (α)).

Adding oil when the fuel is port injected increases the particles emitted in the lowest range-size. Figure 7 shows that the peak of the PSD moves with increase of oil content, starting from 10 nm (with 1% of oil), but never exceeds 35 nm (with 7% of oil). That means that, although a very large amount of oil is released, the detectable particles at the exhaust always fall within the nucleation mode distribution, independently of the way lubricant is added.

In the last case (7% of oil) the granulometric distribution starts to become bi-modal. A second mode appears in the lowest size range, while the main peak is at about 35 nm. This behavior was observed during both CNG and gasoline tests. By looking at Figure 6, it is possible to see that the particles detected during oil injection in motoring conditions belonged to the finest range of the nucleation mode. When oil is at the maximum considered level (Figure 6 (e) and (ε)) in all recorded test repetitions (compare Figure 4 (e) and (ε)) the secondary peak appeared in the same position where the distribution peak was located shortly after that the film was completely formed. This suggests that some oil survived without burning and reached the particle sample point.

Changes were induced to the HC by increasing the lubricant oil amount. In CNG tests the total HC (THC_{c1}) emission level increased because of the increase in Non-Methane-HC, while Methane-HC remained constant in all cases. A maximum increase of 10% (passing from 0 to 7% of oil) was observable in Non-Methane-HC, while the remaining part was more than doubled (150%), which means a total increase of about 40% in HC emissions. When 1% of oil is considered, the total HCs were 6% more than the base-line value.

On the contrary, it should be noted that no significant variations in the levels of CO, CO_2 and NO_x were observed in the tests. The fact that the Non-Methane-HC increased indicates that the oxidation process of the lubricant oil within the combustion chamber was far from complete, especially for the largest oil amounts. As a consequence, the hydrocarbons that constitute the lubricant oil were not converted into CO or CO_2, explaining why no variations were recorded. For the same reason, no noticeable variations were observed in the heat-release and the NO_x, since the oxygen content within the combustion chamber was also practically unchanged. The fact that no appreciable variations were recorded in the heat-release, as well as in the in-cylinder pressure traces, also highlights the inability in distinguishing how much lubricant oil is present in the combustion chamber without performing emissions measurements.

Figure 8 depicts the opacity values recorded during CNG (b) and Gasoline (β) tests and offers a comparison with the corresponding PN total concentration levels (a), (α). The general trends are in good agreement each other and the similarity observed between the two different ways to add lubricant oil to the combustion is also confirmed. The PN suddenly increases by two orders of magnitude as soon as 1% of oil is provided, both in CNG and gasoline operation mode, and then it increases very slightly. The opacity shows a smoother increase, most likely because the emitted particles are too small when the oil content is low and only when their size becomes appreciable do they begin to be detected by the opacimeter.

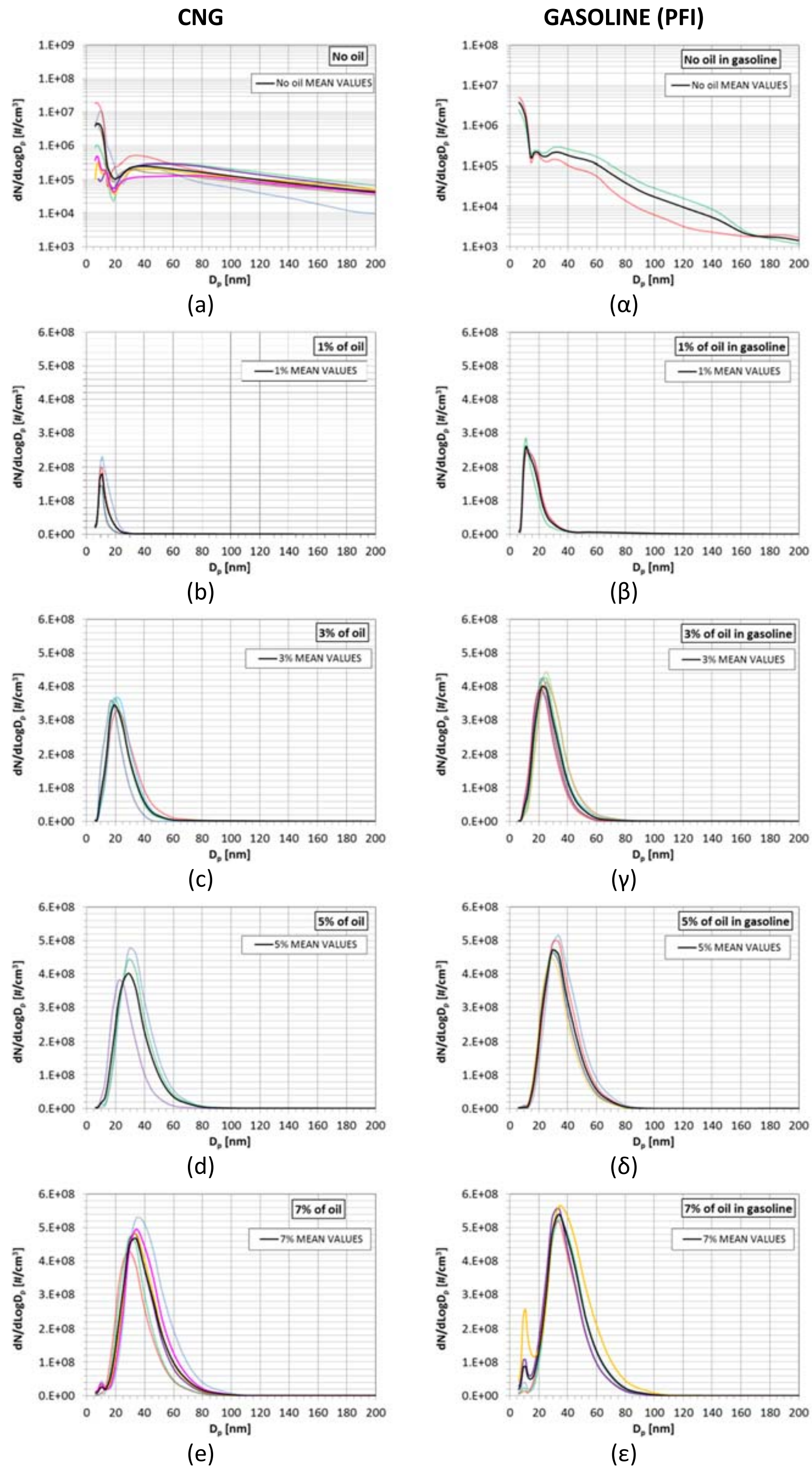

Figure 4 Statistical data concerning the PSD functions measured for both CNG (Latin characters) and gasoline (Greek characters) PFI tests. In each graph, the distributions obtained from each repetition of the same test are reported, together with their calculated mean value (black line). Zero-oil measurements baseline (a) and (α) are reported with a different scale.

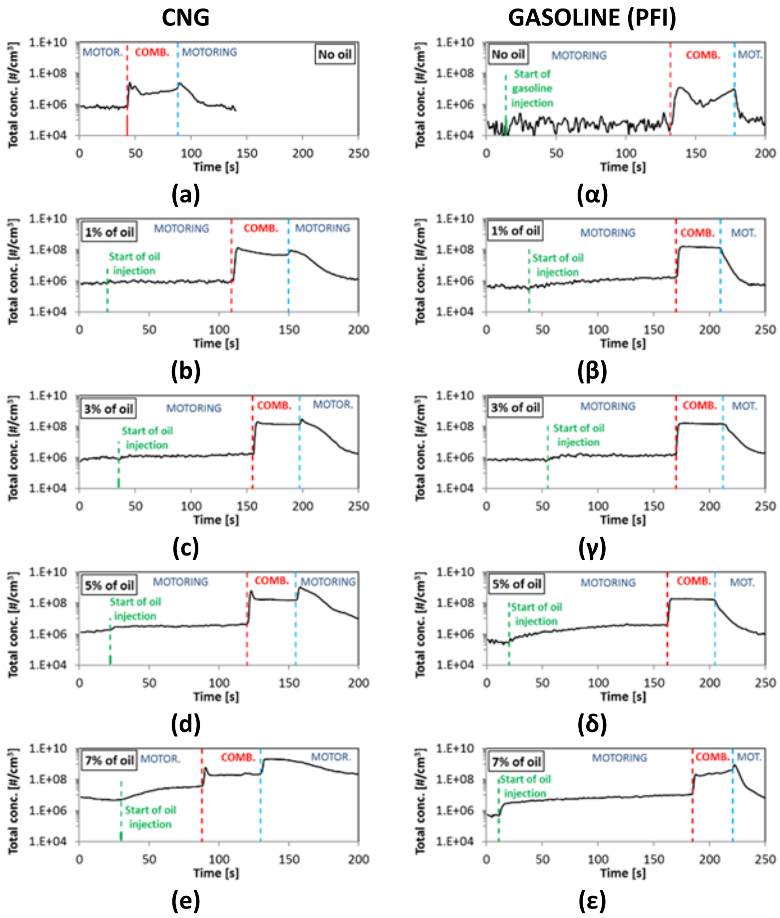

Figure 5 Total concentration number trace evolution with time of one representative case for each explored operating condition, for both the CNG (Latin characters) and gasoline (Greek characters) PFI tests. Green dashed line: start of oil injection into the intake manifold; red dashed line: start of combustion; light blue dashed line: end of combustion.

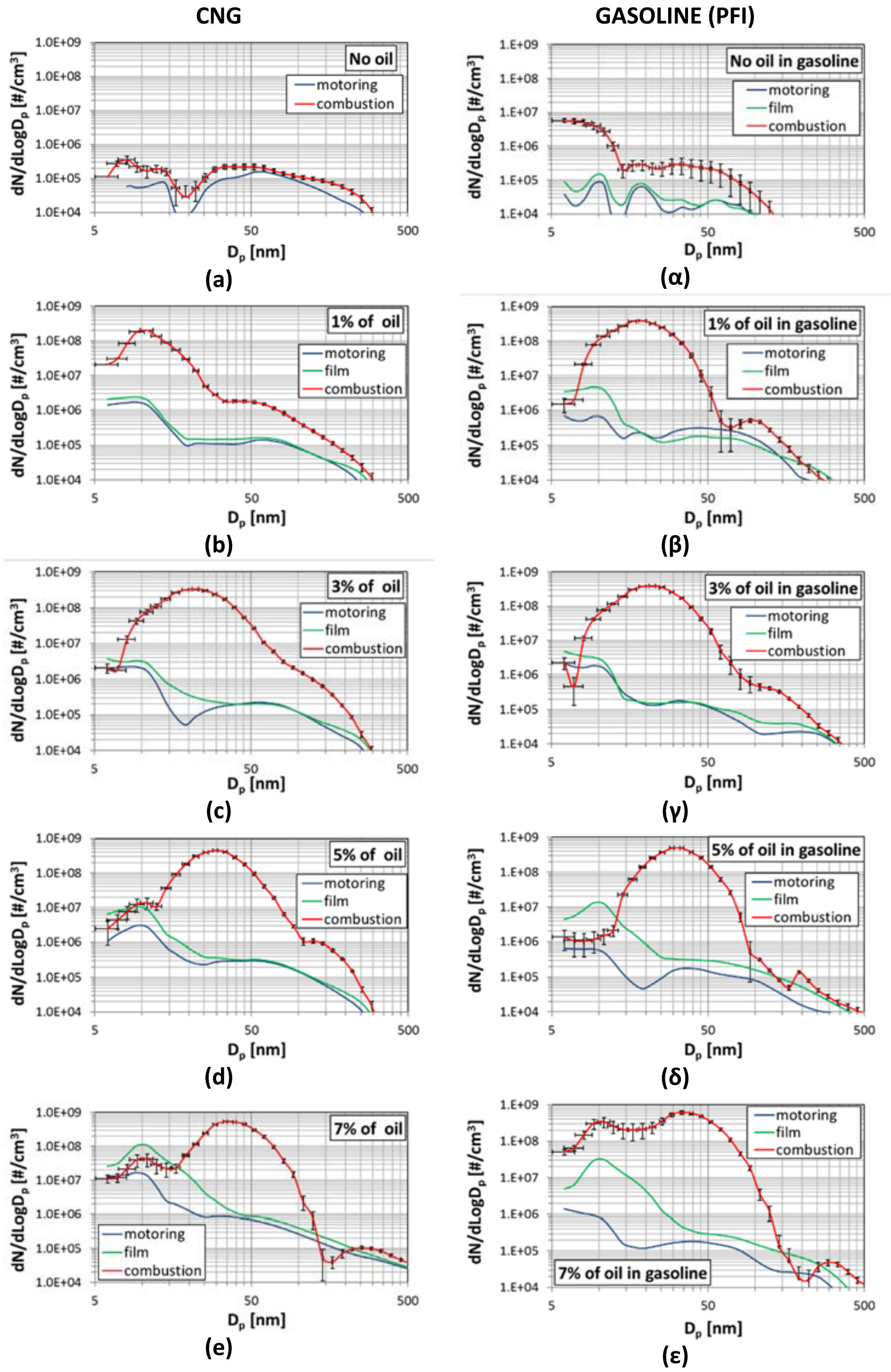

Figure 6 PSD functions for one representative case for each explored operating condition for both the CNG (Latin characters) and gasoline (Greek characters) PFI tests. Light blue line: PSD during motoring conditions; green line: PSD after film forming; red line: PSD during combustion

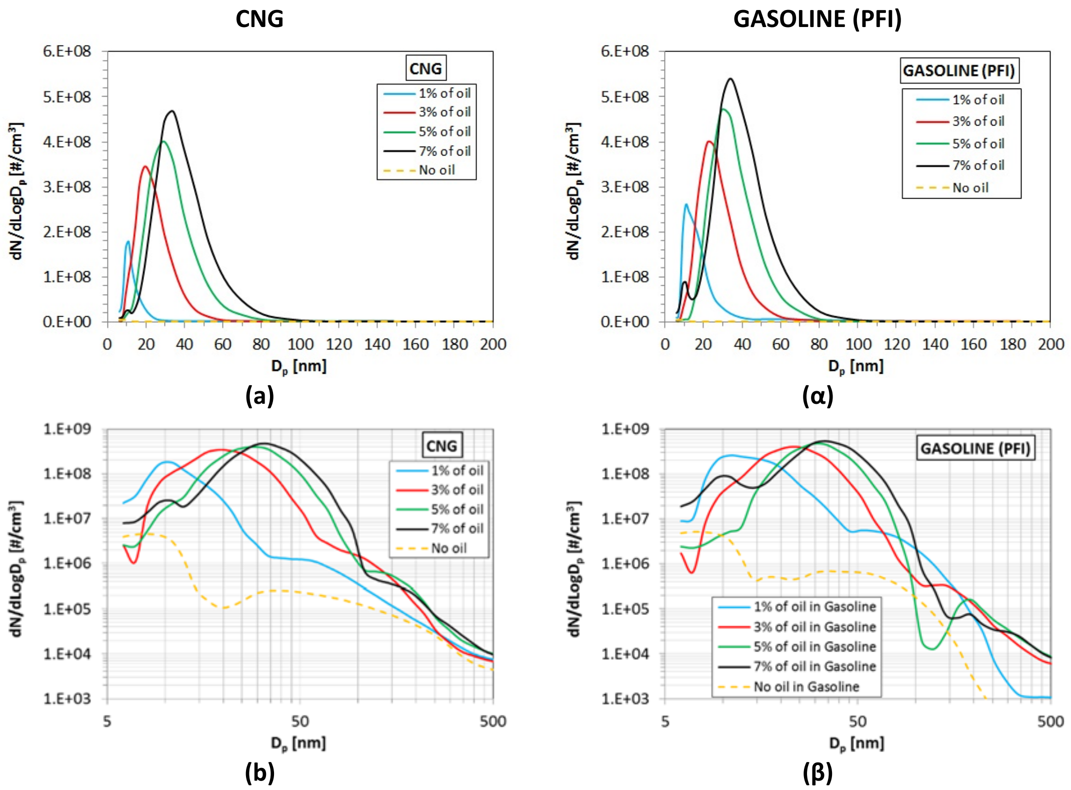

Figure 7 PSD functions (mean values) with a mass lubricant oil content equal to 0% (yellow line), 1% (light blue line), 3% (red line), 5% (green line) and 7% (black line), for both the CNG (Latin characters) and gasoline (Greek characters) PFI tests. For clarity, the data are plotted by using both a linear (a) and (α), and a logarithmic scale (b) and (β).

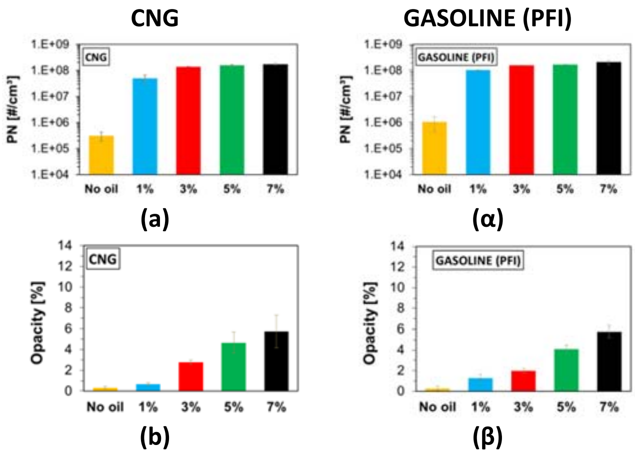

Figure 8 Total concentration number for CNG (a) and gasoline (α); opacity [%] for CNG (b) and gasoline (β) tests.

3.2. DI mode

Results from the experiments in which an oil-gasoline mixture was directly injected into the combustion chamber are first discussed. Then, findings coming from the experiments in which the engine was fueled with CNG in PFI mode and the oil was injected directly into the combustion chamber are examined.

3.2.1. Gasoline DI tests

For the DI tests, the repeatability and stability are summarized in Figure 9, by taking a representative case as example (5% of oil in gasoline). All repetitions are seen to be close to each other (Figure 9 (a)). The PN measurement is very stable (Figure 9 (b)) and consequently the PSD has a well-defined shape (small width of the 95% confidence interval bars in Figure 9 (c)). All others cases presented very similar characteristics and for the sake of brevity, only the mean values are reported in the following discussion.

A comparison between the measured PSDs when the oil content in the direct injected gasoline was changed from 1 to 7%, is reported in Figure 10. As previously done for Figure 7, the data of Figure 10 are plotted by using two different scales for clarity. The formation mechanics of particulate matter is quite different from the PFI case [40]. When no oil was present in gasoline a predominance of particles attributable to the accumulation mode was observable (yellow curve in Figure 10 (b)), in contrast to what was obtained in the PFI tests (yellow curve in Figure 7 (β)).

When oil was added the number of particles falling in the nucleation mode started to be relevant and the shape of the distribution changed. Once again, oil manifested its presence in the lowest range size, but this time the accumulation mode was not negligible. In this case, an increase in the oil content in gasoline also increased the number of particles with sizes larger than 50 nm. This behavior is mainly derived from the soot formation mechanics related to the DI mode. One of the most important aspects related to the soot emission in DI engines is attributable to the fact that some fuel strikes the piston and accumulates as liquid films or pools, which ignite and burn with sooty flames. This is enhanced when an oil-fuel mixture is injected. The poor combustion in pool fires is also responsible for organic particulate, derived either directly from the fuel or from its pyrolysis [30].

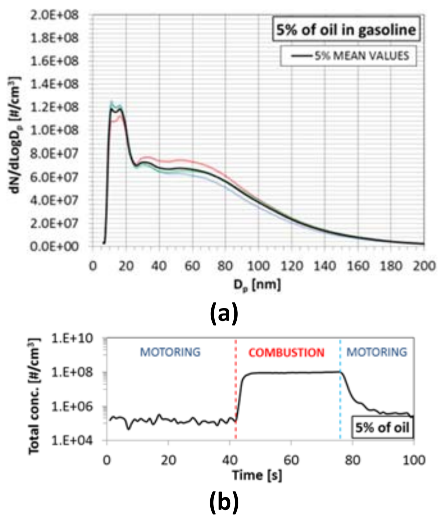

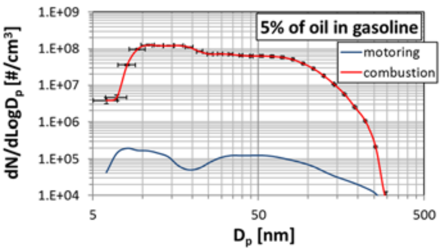

(C)

Figure 9 Statistical PSD functions (a), total concentration number trace evolution with time (b) and PSD functions during motoring conditions and combustion (c) of one representative case (5% of oil) for gasoline DI tests.

Finally, the opacity [%] and the total number of particles detected per cubic centimeter are reported in Figure 11. Because of the larger size of the measured particles, when just gasoline was direct injected (Figure 11 (b) the opacity recorded was 12-times greater than the corresponding PFI value (Figure 8 (β)). The same reason explains why in DI mode the opacity increased much more when lubricant oil was progressively added to gasoline.

3.2.2. Oil DI tests (emulation of oil droplet release with CNG-PFI)

Results from the third way to provide the excess oil are described. These tests emulated droplet release from valve stem seals with oil direct injection and port injected CNG. A relatively large amount of lubricant was released in a short time period.

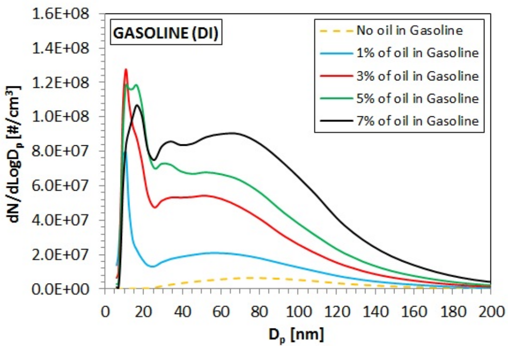

(a)

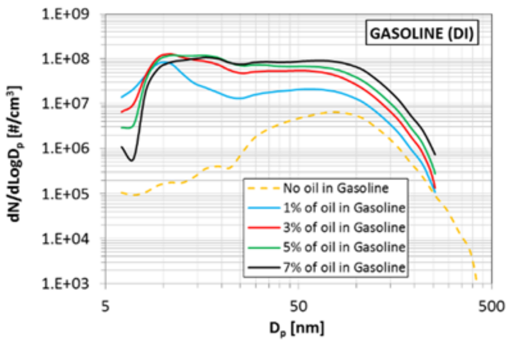

(b)

Figure 10 PSD functions (mean values) with mass lubricant oil content equal to 0% (yellow line), 1% (light blue line), 3% (red line), 5% (green line) and 7% (black line). For clarity, the data are plotted by using both a linear (a) and a logarithmic scale (b).

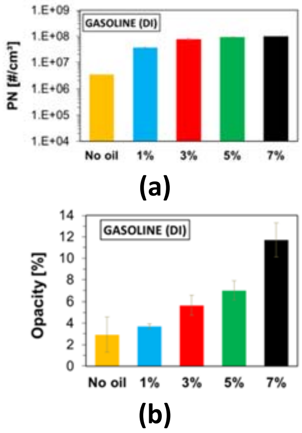

Figure 11 Total concentration number (a) and opacity [%] (b) for gasoline DI tests.

Four repetitions of the tests produced identical results, as depicted in Figure 12. Graph (a) shows that the PN starts to increase as soon as the oil is injected. It reaches a peak level significantly higher than the steady state values and then gradually decreases to the initial steady state level. Figure 12 (c) and (d) provide the time evolution of the PSD function observed during these "transient" measurements, starting a couple of seconds before the start of oil injection. Figure 12 (b) shows that, during the first nine seconds, the total PN increase corresponds to the increase of the smallest size particles. The PSD shape looks more similar to that seen in the gasoline DI tests (in which a lubricant-fuel mixture was injected directly into the combustion chamber) rather than that observed during the CNG tests (when the oil was injected into the intake manifold as a mist). Figure 12 (b) shows that the distribution takes on goes back to its original shape before the oil injection start.

These findings highlight that the way the oil reaches the combustion chamber characterizes the particle emission dynamics. Oil always increases the number of very small particles; and in fact, even when the lubricant amount is quite large, particles exceeding 50 nm appear in appreciable quantities only if the oil is injected directly into the combustion chamber so that it can survive as liquid droplets.

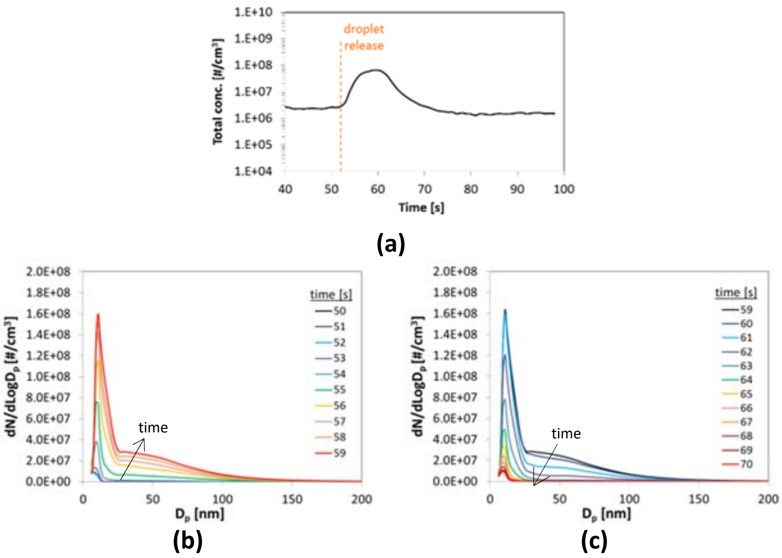

Figure 12 Total concentration number trace evolution with time (a) and PSD time evolution during the first 9 seconds (b) and the subsequent 10 seconds (c), for emulation of oil droplet release.

4. CONCLUSIONS

An extensive experimental investigation was conducted to provide insights about the effects of lubricant oil on particle emissions from both gasoline and CNG SI engines. Three different strategies to provide the additional lubricant oil and two combustion modes (PFI and DI) were investigated. When gasoline was used as fuel, a fuel-oil mixture was either port- or direct-injected. When the engine was fueled with CNG, the oil was either injected into the intake flow or directly into the engine combustion chamber, while port injected CNG was provided as fuel. This last strategy aimed at simulating droplet release from valve stem seals.

The optically accessible engine was run without lubrication. A dedicated oil injection line, coupled with an early lubricant oil injection (oil injection started when the engine was motored) allowed stable and repeatable measurements of the particle emissions, despite the very short available test time. Lubricant oil was 1, 3, 5 and 7% of the fuel mass and the results were compared with the "oil-free" condition for each fuel and injection mode considered.

In all of the experimental arrangements, oil addition produced a significant increase of very small particles emitted. When oil was fed to the intake manifold, both by itself and blended with fuel, the peak of the PSD function increased with the oil content, starting from 10 nm (with 1% of oil), but it never exceeded 35 nm (with 7% of oil).

When no oil was present in the direct injected gasoline, a predominance of particles attributable to the accumulation mode was observed, in contrast to what obtained in PFI mode, as expected with Diesel-like conditions favoring the generation of larger soot particles. When an oil-gasoline mixture was considered in the DI tests, particles with the finest size started to appear and began to predominate. However, in this case, an increase in oil content also led to an increase in the number of particles with sizes larger than 50 nm. This behavior was mainly attributable to the fact that what was seen when just gasoline was direct injected is now enhanced by the presence of lubricant.

The emulation of the droplet release coming from the valve-stem seals was experimentally realized by providing the excess oil directly into the combustion chamber during CNG (PFI) combustion. The PSD function presented a shape more similar to that seen in the gasoline DI tests, rather than that observed during the CNG tests, in which the oil was entrained in the intake manifold.

With lubricant oil addition, no significant variations in engine-out CO, CO_2 and NO_x were observed. However, in the CNG tests the total HC emission levels increased because of the increase in Non-Methane-HC, while Methane-HC remained constant in all cases. This indicated that the oil was not completely oxidized within the combustion chamber. In addition, in both gasoline and CNG (PFI) tests, the PN suddenly increased by roughly two orders of magnitude when 1% of oil was provided. The opacity measurements showed a smoother trend, most likely because the emitted particles were too small for the opacimeter when the oil content was low. This also explained why the opacity number, recorded when just gasoline was direct injected, was 12-times greater than the corresponding value in the PFI mode.

It was found that oil addition always produced a remarkable increase of the finest particles. This finding is in agreement with previous research in which it was shown that lubricant oil assumes the aspect of an exhaust aerosol having log normal-size distributions with geometric mean diameters that never exceed 30 nm. In addition, the present results confirm findings from other studies in which it was supposed that the larger oil consumption seen during accelerations might be associated with the great amount of nucleation mode particles released from CNG SI engines during accelerations. In the present work, a noticeable amount of accumulation mode particles was seen only when lubricant oil was directly injected into the combustion chamber, and this proves that the way lubricant oil reaches the combustion chamber does affect the dynamics of particle emissions formation whether it is blended or not with the fuel. Further improvements of the designed oil injection line would allow the possibility to inject even less oil than the minimum level of 1% considered in this study. In addition, tests with different lubricant composition could also further establish the influence of oil characteristics on soot emissions. A further investigation of the effect that different additional dilutions of the exhaust sample can produce on the results is also needed, since the volatile part of the recorded particle emissions can play a significant role. In addition, exploiting the optical accessibility of the engine will also provide very useful additional information. Therefore, separate tests will be performed in which changes in the apparent luminosity will be recorded, as well as OH* and CH* will be detected by means of UV-visible spectroscopy and images of the oil injection will be recorded.

AKNOWLEDGMENTS

The authors are grateful to Carlo Rossi and Bruno Sgammato, for their invaluable technical support during the entire experimental campaign.

REFERENCES

[1] Shimasaki Y, Kobayashi M, Sakamoto H, Ueno M, Hasegawa M, Yamaguchi S, Suzuki T. Study on engine management system using in-cylinder pressure sensor integrated with spark plug. SAE Technical Paper; 2004 Mar 8.

[2] Amirante R, Casavola C, Distaso E, Tamburrano P. Towards the Development of the In-Cylinder Pressure Measurement Based on the Strain Gauge Technique for Internal Combustion Engines. SAE Technical Paper; 2015 Sep 6.

[3] Myung CL, Park S. Exhaust nanoparticle emissions from internal combustion engines: A review. International Journal of Automotive Technology. 2012 Jan 1;13(1):9-22.

[4] Bischof OF. Recent Developments in the Measurement of Low Particulate Emissions from Mobile Sources: A Review of Particle Number Legislations. Emission Control Science and Technology. 2015;1(2):203-12.

[5] Jacobs L, Nawrot TS, De Geus B, Meeusen R, Degraeuwe B, Bernard A, Sughis M, Nemery B, Panis LI. Subclinical responses in healthy cyclists briefly exposed to traffic-related air pollution: an intervention study. Environmental Health. 2010 Oct 25;9(1):64.

[6] Su DS, Serafino A, Müller JO, Jentoft RE, Schlögl R, Fiorito S. Cytotoxicity and inflammatory potential of soot particles of low-emission Diesel engines. Environmental science & technology. 2008 Jan 25;42(5):1761-5.

[7] Brugge D, Durant JL, Rioux C. Near-highway pollutants in motor vehicle exhaust: a review of epidemiologic evidence of cardiac and pulmonary health risks. Environmental Health. 2007 Aug 9;6(1):23.

[8] Pope III CA, Dockery DW. Health effects of fine particulate air pollution: lines that connect. Journal of the air & waste management association. 2006 Jun 1;56(6):709-42.

[9] Riediker M, Cascio WE, Griggs TR, Herbst MC, Bromberg PA, Neas L, Williams RW, Devlin RB. Particulate matter exposure in cars is associated with cardiovascular effects in healthy young men. American journal of respiratory and critical care medicine. 2004 Apr 15;169(8):934-40.

[10] Lave LB, Maclean HL. An environmental-economic evaluation of hybrid electric vehicles : Toyota's Prius vs its conventional internal combustion engine Corolla. Transp Res Part D Transp Environ 2002;7:155–62.

[11] Amirante R, Cassone E, Distaso E, Tamburrano P. Overview on recent developments in energy storage: Mechanical, electrochemical and hydrogen technologies. Energy Convers Manag 2017;132:372–87.

[12] Amirante R, Tamburrano P. Novel, cost-effective configurations of combined power plants for small-scale cogeneration from biomass: Feasibility study and performance optimization. Energy Convers Manag 2015;97:111–20.

[13] Amirante R, Tamburrano P. Novel, cost-effective configurations of combined power plants for small-scale cogeneration from biomass: Feasibility study and performance optimization. Energy Convers Manag 2015;97:111–20.

[14] Haycock R, Caines AJ, Haycock RF, Hillier JE. Automotive lubricants reference book. John Wiley & Sons; 2004.

[15] Gidney JT, Twigg MV, Kittelson DB. Effect of organometallic fuel additives on nanoparticle emissions from a gasoline passenger car. Environmental science & technology. 2010 Mar 1;44(7):2562-9.

[16] Thiruvengadam A, Besch MC, Yoon S, Collins J, Kappanna H, Carder DK, Ayala A, Herner J, Gautam M. Characterization of Particulate Matter Emissions from a Current Technology Natural Gas Engine. Environmental science & technology. 2014 Jul 3;48(14):8235-42.

[17] McGeehan JA, Yeh S, Couch M, Hinz A, Otterholm B, Walker A, Blakeman P. On the road to 2010 emissions: field test results and analysis with DPF-SCR system and ultra low sulfur Diesel fuel. SAE Technical Paper; 2005 Oct 24.

[18] Cheung KL, Ntziachristos L, Tzamkiozis T, Schauer JJ, Samaras Z, Moore KF, Sioutas C. Emissions of particulate trace elements, metals and organic species from gasoline, Diesel, and bioDiesel passenger vehicles and their relation to oxidative potential. Aerosol Science and Technology. 2010 Jun 4;44(7):500-13.

[19] Lee DG, Miller A, Park KH, Zachariah MR. Effects of trace metals on particulate matter formation in a Diesel engine: Metal contents from ferrocene and lube oil. International journal of automotive technology. 2006 Oct;7(6):667-73.

[20] Duffin R, Tran L, Brown D, Stone V, Donaldson K. Proinflammogenic effects of low-toxicity and metal nanoparticles in vivo and in vitro: highlighting the role of particle surface area and surface reactivity. Inhalation toxicology. 2007 Jan 1;19(10):849-56.

[21] Wilson MR, Lightbody JH, Donaldson K, Sales J, Stone V. Interactions between ultrafine particles and transition metals in vivo and in vitro. Toxicology and applied pharmacology. 2002 Nov 1;184(3):172-9.

[22] Donaldson K, Tran L, Jimenez LA, Duffin R, Newby DE, Mills N, MacNee W, Stone V. Combustion-derived nanoparticles: a review of their toxicology following inhalation exposure. Particle and fibre toxicology. 2005 Oct 21;2(1):10.
[23] Skillas G, Qian Z, Baltensperger U, Matter U, Burtscher H. The influence of additives on the size distribution and composition of particles produced by Diesel engines. Combustion science and Technology. 2000 May 1;154(1):259-73.
[24] Jung H, Kittelson DB, Zachariah MR. The influence of a cerium additive on ultrafine Diesel particle emissions and kinetics of oxidation. Combustion and Flame. 2005 Aug 31;142(3):276-88.
[25] Kasper M, Sattler K, Siegmann K, Matter U, Siegmann HC. The influence of fuel additives on the formation of carbon during combustion. Journal of Aerosol Science. 1999 Feb 1;30(2):217-25.
[26] Jung H, Kittelson DB, Zachariah MR. The influence of engine lubricating oil on Diesel nanoparticle emissions and kinetics of oxidation. SAE Technical Paper; 2003 Oct 27.
[27] Miller AL, Stipe CB, Habjan MC, Ahlstrand GG. Role of lubrication oil in particulate emissions from a hydrogen-powered internal combustion engine. Environmental science & technology. 2007 Oct 1;41(19):6828-35.
[28] Sonntag DB, Bailey CR, Fulper CR, Baldauf RW. Contribution of lubricating oil to particulate matter emissions from light-duty gasoline vehicles in Kansas City. Environmental science & technology. 2012 Mar 14;46(7):4191-9.
[29] Pirjola L, Karjalainen P, Heikkilä J, Saari S, Tzamkiozis T, Ntziachristos L, Kulmala K, Keskinen J, Rönkkö T. Effects of Fresh Lubricant Oils on Particle Emissions Emitted by a Modern Gasoline Direct Injection Passenger Car. Environmental science & technology. 2015 Feb 26;49(6):3644-52.
[30] Eastwood P. Particulate emissions from vehicles. John Wiley & Sons; 2008 Apr 15.
[31] De Petris C, Giglio V, Police G. Some insights on mechanisms of oil consumption. SAE Technical Paper; 1996 May 1.
[32] Yilmaz E, Thirouard B, Tian T, Wong VW, Heywood JB, Lee N. Analysis of Oil Consumption Behavior during Ramp Transients in a Production Spark Ignition Engine. SAE Technical Paper; 2001 Sep 24.
[33] Graskow BR, Kittelson DB, Abdul-Khalek IS, Ahmadi MR, Morris JE. Characterization of exhaust particulate emissions from a spark ignition engine. SAE Technical Paper; 1998 Feb 23.
[34] Tonegawa Y, Oguchi M, Tsuchiya K, Sasaki S, Ohashi T, Goto Y. Evaluation of Regulated Materials and Ultra Fine Particle Emission from Trial Production of Heavy-Duty CNG Engine. SAE Technical Paper; 2006 Oct 16.
[35] Jayaratne ER, Meyer NK, Ristovski ZD, Morawska L, Miljevic B. Critical analysis of high particle number emissions from accelerating compressed natural gas buses. Environmental science & technology. 2010 Apr 12;44(10):3724-31.
[36] Amirante R, Distaso E, Tamburrano P, Reitz RD. Measured and Predicted Soot Particle Emissions from Natural Gas Engines. SAE Technical Paper; 2015 Sep 6.
[37] Stanglmaier, R. H., Li, J., & Matthews, R. D. (1999). *The effect of in-cylinder wall wetting location on the HC emissions from SI engines* (No. 1999-01-0502). SAE Technical Paper.
[38] Di Iorio S, Sementa P, Vaglieco BM. Experimental investigation on the combustion process in a spark ignition optically accessible engine fueled with methane/hydrogen blends. International Journal of Hydrogen Energy. 2014 Jun 15;39(18):9809-23.
[39] Sutton M, Britton N, Otterholm B, Tengström P, Frennfelt C, Walker A, Murray I. Investigations into lubricant blocking of Diesel particulate filters. SAE Technical Paper; 2004 Oct 25.
[40] Di Iorio S, Sementa P, Vaglieco BM. Experimental Characterization of an Ethanol DI-Gasoline PFI and Gasoline DI-Gasoline PFI Dual Fuel Small Displacement SI Engine. SAE Technical Paper; 2015 Apr 14.

APPENDIX I

Notation

Ba	Barium
C_2H_6	Ethane
C_3H_8	Propane
Ca	Calcium
CH_4	Methane
CO	Carbon monoxide
CO_2	Carbon dioxide

Cu Copper
Fe Iron
HC Hydrocarbons
Mg Magnesium
Mn Manganese
N_2 Nitrogen
Ni Nickel
NO_x Nitrogen oxides
P Phosphorus
Zn Zinc

Abbreviations

CAD Crank Angle Degree
CFD Computational Fluid Dynamics
CNG Compressed Natural Gas
DI Direct Injection
DOI Duration of Injection
DPF Diesel Particulate Filter
PAH Poly-Aromatic Hydrocarbon
PFI Port Fuel Injection
PM Particulate Matter
PMP Particle Measurement Programme
PN Particulate Number
PSD Particle Size Distribution
TDC Top Dead Center
THC Total Hydrocarbons
TWC Three-Way Catalyst